

PROCEEDINGS OF SPIE

[SPIDigitalLibrary.org/conference-proceedings-of-spie](https://spiedigitallibrary.org/conference-proceedings-of-spie)

Real-time three-dimensional temperature mapping in photothermal therapy with optoacoustic tomography

Francisco Javier Oyaga Landa
Xosé Lu s De n-Ben
Ronald Sroka
Daniel Razansky

Real-time Three-dimensional Temperature Mapping in Photothermal Therapy with Optoacoustic Tomography

Francisco Javier Oyaga Landa,^{1,2} Xosé Luís Deán-Ben,¹ Ronald Sroka,³ and Daniel Razansky^{1,2,*}

¹Institute for Biological and Medical Imaging (IBMI), Helmholtz Center Munich, Neuherberg, Germany

²Faculty of Medicine, Technical University of Munich, Germany

³Laser Research Laboratory/LIFE Center, Ludwig-Maximilian-University, Munich, Germany

*Corresponding author: dr@tum.de

Abstract: Ablation and photothermal therapy are widely employed medical protocols where the selective destruction of tissue is a necessity as in cancerous tissue removal or vascular and brain abnormalities. Tissue denaturation takes place when the temperature reaches a threshold value while the time of exposure determines the lesion size. Therefore, the spatio-temporal distribution of temperature plays a crucial role in the outcome of these clinical interventions. We demonstrate fast volumetric temperature mapping with optoacoustic tomography based on real-time optoacoustic readings from the treated region. The performance of the method was investigated in tissue-mimicking phantom experiments. The new ability to non-invasively measure temperature volumetrically in an entire treated region with high spatial and temporal resolutions holds potential for improving safety and efficacy of thermal ablation and to advance the general applicability of laser-based therapy.

Keywords: Ablation of Tissue; Optoacoustic imaging; Optoacoustic Tomography; Temperature.

Introduction

Thermal ablation procedures are widely employed in clinical interventions such as in selective ablation of cancerous tissues, benign hyperplasias or varicose veins as well as in the treatment of cardiac arrhythmias and enhanced drug delivery [1-6]. Thermal ablation procedures can be classified depending on the heat source used. Laser light, focused ultrasound, radio-frequency current and microwaves are commonly employed [2]. Laser-induced thermotherapy (LITT), also known as laser ablation, has gained popularity due to its advantages, such as reduced treatment times, minimal invasiveness and low hardware investment [3, 4]. LITT is carried out employing laser radiation as energy source, usually guided through optic fibers.

Heat-driven denaturation generally takes place when tissues are heated above 50°C, while the exposure time further determines the size of the induced lesion. Therefore, the spatio-temporal temperature distribution in the treated tissue plays a crucial role in the outcome of photothermal interventions. On the other hand, several therapeutic procedures use lower temperature elevations without inducing irreversible tissue damage, including local and whole-body hyperthermia [7] as well as low- and medium-intensity focused ultrasound [8, 9]. The effectiveness of thermal therapies heavily relies on the ability to accurately monitor and control the volumetric temperature distribution of the treated tissues in real time [2]. Invasive approaches based on thermocouples or fiber-optic sensors [10] can be used for temperature monitoring, which can only capture temperature values in a few locations within the heated region. The temperature map can be obtained using non-invasive imaging modalities, such as infrared thermometry [11], ultrasound [12], x-ray computed tomography (CT) [13] or magnetic resonance imaging (MRI) [14]. Nevertheless, these techniques are either limited by low penetration, sensitivity, contrast or otherwise lack an adequate temporal resolution for dynamic mapping of the temperature fields.

In this work, optoacoustic imaging is suggested as an advantageous approach for monitoring photothermal therapy that offers high sensitivity to temperature fluctuations [15-17]. Previous works have established the dependence of the optoacoustic signal during thermal therapies [18-23]. Yet, no real-time mapping of the temperature field in three-dimensions has been so far demonstrated. We study herein the performance of optoacoustics to dynamically map temperature in the treated tissue.

Methods

Optoacoustic image acquisition set-up and reconstruction

Figure 1 depicts the lay-out of the experimental setup. The ablation fiber heated the tissue through a diode laser providing 20W of continuous wave power at 830 nm (Indigo 830, Indigo Medical Inc., Lawrenceville, New Jersey).

A specialized fiberoptic delivery system with a cylindrical diffuser at the tip was used to guide the ablation beam to the region of interest. Dynamic volumetric temperature monitoring was performed with a three-dimensional optoacoustic probe made of a 512-element spherical transducer array covering an angle 140° with 4 cm radius of curvature (1.3π solid angle). The individual elements of the array have a central frequency of 5 MHz and 100% detection bandwidth, corresponding to nearly isotropic imaging resolution of $\sim 150 \mu\text{m}$ around the geometrical center of the sphere. Acoustic coupling was ensured by molding agarose gel between the active surface and the surface of the imaged sample (Figure 1). Optoacoustic responses were excited with a short-pulsed ($<10 \text{ ns}$) laser source (Innolas Laser GmbH, Krailling, Germany) guided via a custom-made fiber bundle (CeramOptec GmbH, Bonn, Germany) through a hollow cylindrical cavity in the center of the array. For imaging, the wavelength of the tunable optoacoustic laser source was also set to 830 nm and the optical fluence was roughly 11 mJ/cm^2 at the surface of the imaged sample. The pulse repetition frequency (PRF) of the laser was set to 5 Hz. A second arm of the fiber bundle was guided to a powermeter (EM-USB-J-25MB-LE, Coherent Inc., Santa Clara, California) to monitor the energy per pulse, which was used to normalize the acquired signals. All 512 OA signals were simultaneously digitized at 40 mega-samples per second (MSPS) by a custom-made data acquisition (DAQ) system (Falkenstein Mikrosysteme GmbH, Taufkirchen, Germany) triggered with the Q-switch output of the laser.

Optoacoustic images were lately reconstructed with a graphics processing unit (GPU)-based three-dimensional back-projection algorithm [24]. Before reconstruction, the acquired signals were deconvolved with the impulse response of the array elements and band-pass filtered between 0.1 MHz and 7 MHz.

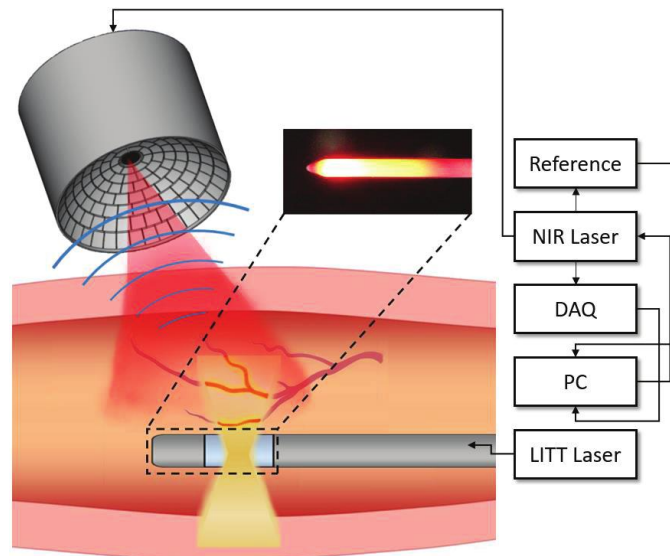


Fig. 1. Lay-out of the experimental setup.

Temperature Estimation Method

Our proposed optoacoustic temperature estimation method is based on the temperature dependence of the optoacoustic signals. When the optoacoustic responses are excited with a short-duration laser pulse, the so-called thermal and stress confinement conditions can be assumed [25]. Under these conditions, the initial OA signal (pressure) is given by $p_0 = \Gamma \mu_a \Phi$, being Γ the (dimensionless) Grüneisen parameter, μ_a the optical absorption coefficient and Φ the light fluence. The temperature dependence of the generated OA signals mainly comes from variations in the Grüneisen parameter. The temperature dependence of the Grüneisen parameter in water-like aqueous media can be approximated by [25]

$$\Gamma(T) = 0.0043 + 0.0053T, \quad (1)$$

where T is expressed in $^\circ\text{C}$. Eq. (1) describes temperature dependence of the Grüneisen parameter for water and diluted aqueous solutions [26]. The relative change of the OA signal as a function of the temperature increase ΔT can be then expressed as

$$\frac{\Delta p_0}{p_{0,0}} = \frac{0.0053 \Delta T}{0.0043 + 0.0053 \cdot T_0}, \quad (2)$$

being $p_{0,0}$ and T_0 the initial (baseline) optoacoustic signal and the initial temperature before the ablation experiment, respectively. According to Eq. 2, the amplitude of the OA signals is expected to increase by approximately 2.7% per degree for typical temperature values of 36°C in living organisms. We further define F as the ratio between the relative increment of the OA signal and the relative increment of temperature, i.e.,

$$F = \frac{T_0}{p_{0,0} \Delta T} \Delta p_0 \quad (3)$$

Considering Eq. 2, the theoretical value of F (F_{th}) can be expressed as a function of the initial temperature T_0 via

$$F_{th} = \left(\frac{0.8113}{T_0} + 1 \right)^{-1} \quad (4)$$

The temperature increment can then be retrieved from the relative OA signal increase as

$$\Delta T = \frac{T_0}{p_{0,0} F} \Delta p_0 \quad (5)$$

It should be noticed that, for temperatures exceeding 50°C, cell denaturation and coagulation mechanisms are known to take place in soft biological tissues, introducing non-linear variations of the Grüneisen parameter [21] as well as modifications in the optical absorption and scattering coefficient of the ablated tissues [27]. Accuracy of the above temperature estimation method is thus expected to be limited to the temperatures range lying below the coagulation threshold.

Phantom validation experiments

The quantitative accuracy of the temperature monitoring approach according to Eq. 5 was tested in a tissue-mimicking phantom. In these experiments, three tubings with 1 mm diameter and 10 mm length were embedded in a ~8 mm layer of chicken breast. The tubings were filled with murine blood and sealed with glue. Three thermocouples (Physitemp Instruments Inc., Clifton, New Jersey) were inserted into the tubings to provide real-time temperature values. The thermocouple readings were digitized with an embedded NI 9213 DAQ (National Instruments Corporation, Austin, Texas, U.S.). For each tubing, the temperature estimations were retrieved from the known region of interest (ROI) where the thermocouple sensors were located.

Results

Tissue-mimicking phantom experiments

Figure 2 shows the reconstructed optoacoustic images at three different instants during the laser heating process. The ablation fiber was positioned in parallel to the tubings at 5 mm from the leftmost tubing. The progressive increment in the OA signal as temperature increases can be perceived in all tubings (Figures 2a-c). The temperature increase in murine blood was then obtained from Eq. 5, where the F factor is calculated through Eq. 4. The estimated temperature increase inside the three tubings is plotted in Figure 2d as dashed lines. For calculating the relative signal increments, the baseline optoacoustic image was taken as the average of 50 frames before the ablation procedure. The temperature increase values, readings from the thermocouples located at the same ROIs, are also shown in Figure 2d as continuous lines.

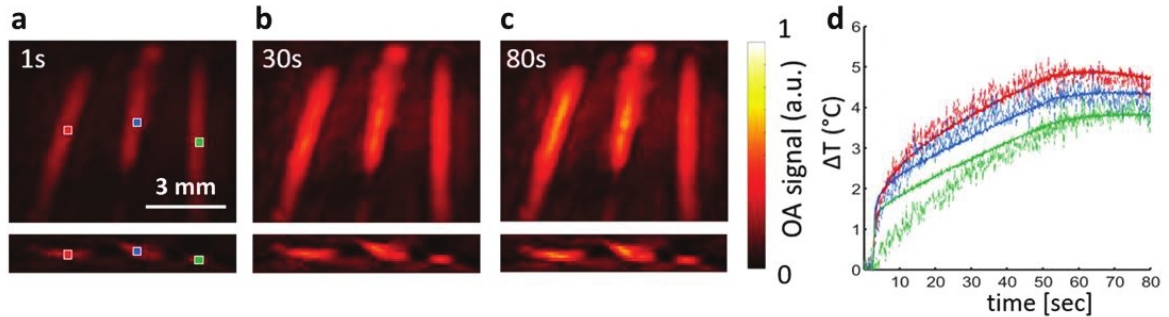


Fig. 2. Optoacoustic temperature estimations in a tissue-mimicking phantom. (a)-(c) Transverse and coronal maximum intensity projection (MIP) optoacoustic images reconstructed for three different time points during laser heating of the phantom; (d) The temperature increase estimated from the optoacoustic signal variations (dashed curves) as compared to the temperature increase measured with thermocouples (solid curves). The regions of interest considered for the estimation are marked in panel (a).

As expected, lower temperature increments result in larger disagreement between the optoacoustically-estimated temperature values and those measured with the thermocouples. These deviation can be partially attributed to the relative uncertainty in the measured Δp_0 values (see Eq. 3), originating from the noise in optoacoustic measurements. Note however that the discrepancy may also result from inaccuracies in the theoretical F values that were calculated using Eq. 4 assuming a homogenous water medium. Further uncertainty can be originated from the location of the thermocouple tip.

Discussion

The lack of simple and reliable non-invasive temperature feed-back represents a major barrier towards broader adaptation of laser-based thermotherapy procedures in pre-clinical research and clinical routine. The presented results showcase that volumetric optoacoustic imaging may emerge as a promising tool for quantitative monitoring of the temperature field during thermal therapies. Optoacoustics is particularly suitable for this purpose due to its high sensitivity to temperature changes as well as the powerful ability to represent the temperature changes in an entire treated volume with both high spatial and temporal resolutions in the $150\mu\text{m}$ and 10ms ranges, respectively.

Note that in the experiments performed, the temperature dependence of the Grüneisen parameter was adopted from an empirical formula for diluted aqueous solutions, which may not accurately represent the physical reality in soft biological tissues [21]. Thus, accurate calibration of this parameter in different tissues may result in better accuracy when estimating the temperature-dependence of the OA signals. In addition, accuracy of the temperature estimations has been shown to be directly linked to the contrast and noise levels of the reconstructed optoacoustic images while the average optoacoustic signal strength is expected to drop by approximately an order of magnitude for each centimeter of penetration in living tissues at the near-infrared wavelengths [25]. In the current study, temperature estimations were achieved at up to 10 mm depth in *ex-vivo* mouse tissues without employing signal averaging. For monitoring at deeper locations, one potential solution may involve guiding the optoacoustic excitation beam through the same fiber used for delivering the ablation beam. In this way, since both optoacoustic imaging and laser ablation are usually performed in the near-infrared wavelength range, an even higher level of hardware integration could be potentially achieved if the same laser is used for both ablation and generation of optoacoustic responses.

The amount of monitored information can be enhanced by acquisition of multispectral optoacoustic tomography (MSOT) data [29]. Since MSOT enables identifying spectral variations in the imaged tissue, this information may further help improving the accuracy of the suggested temperature monitoring approach by recognizing alterations in the optical or chemical parameters of the imaged tissue resulting from e.g. tissue coagulation.

In the present investigation, the underlying modeling assumption was that the tissue optical properties remain unchanged during the heating process, which is not the case if tissue coagulation or other irreversible thermal damage occur. It has been previously observed that a stronger and non-linear dependence of the optoacoustic signal intensity on temperature was produced in tissues heated above 53°C [21]. In addition, not only the Grüneisen parameter but several other physical parameters, such as optical absorption and scattering, are altered due to tissue coagulation [27]. Consequently, real-time computation of the optoacoustic inversion and thermal diffusion in three and four dimensions become much more complex and it another mathematical approach in the future.

During *in-vivo* thermal therapy procedures, it is anticipated that blood perfusion will play a dominant role in thermal diffusion effects. Whereas the OA signal might be influenced by the bigger presence of blood volume that can lead to higher inaccuracies between the actual temperature values and the OA estimations. Also, increased blood perfusion has a cooling effect [30, 31] that should have to be taken into account in order to avoid further inaccuracies from the thermal diffusion model.

Conclusion

In conclusion, we developed a novel high resolution volumetric temperature monitoring method during photothermal therapy based on real-time acquisition of three-dimensional optoacoustic data. The present results suggest that the proposed method enables mapping the temperature field distribution during laser-induced thermal therapy. It is expected that the proposed temperature estimation approach improves the safety and efficacy of photothermal treatments and its general applicability in common clinics.

Acknowledgements

The authors acknowledge support from the German Research Foundation (DFG) under Research Grant RA 1848/5-1.

References

- [1] Moros, E.G. Physics of thermal therapy: fundamentals and clinical applications. *CRC Press*, (2012).
- [2] Chu, K.F. & Dupuy, D.E. Thermal ablation of tumours: biological mechanisms and advances in therapy. *Nature Reviews Cancer*. **14**, 199-208 (2014).
- [3] Mensel, B., Weigel, C. & Hosten, N. Laser-induced thermotherapy. Minimally invasive tumor therapies. *Springer Berlin Heidelberg*. 69-75 (2006).
- [4] Torres-Reveron, J., Tomaszewicz, H.C., Shetty, A., Amankulor, N.M. & Chiang, V.L. Stereotactic laser induced thermotherapy (LITT): a novel treatment for brain lesions regrowing after radiosurgery. *Journal of neuro-oncology*. **113**, 495-503 (2013).
- [5] Ke, H. et al. Gold nanoshelled liquid perfluorocarbon magnetic nanocapsules: a nanotheranostic platform for bimodal ultrasound/magnetic resonance imaging guided photothermal tumor ablation. *Theranostics*. **14**, 12-23 (2014).
- [6] Zhang, F. et al. Noninvasive dynamic imaging of tumor early response to nanoparticle-mediated photothermal therapy. *Theranostics*. **5**, 1444-1455 (2015).
- [7] Datta, N. R. et. al. Local hyperthermia combined with radiotherapy and/or chemotherapy: Recent advances and promises for the future. *Cancer Treatments Reviews*. **41**, 742-753 (2015).
- [8] Bandyopadhyay, S. et. al. Low-Intensity focused ultrasound induces reversal of tumor-induced T Cell tolerance and prevents immune escape. *The Journal of Immunology*. **196**, 1964-1976 (2016).
- [9] Shaw, A., Haar, G.T., Haller, J. & Wilkens, V. Towards a dosimetric framework for therapeutic ultrasound. *International Journal of Hyperthermia*. **31**(2), 182-192 (2015).
- [10] Saccomandi, P., Schena, E. & Silvestri, S. Techniques for temperature monitoring during laser-induced thermotherapy: An overview. *International Journal of Hyperthermia*. **29**, 609-619 (2013).
- [11] Lahiri, B. B., Subramainam, B., Jayakumar, T. & Philip, J. Medical applications of infrared thermography: A review. *Infrared Physics & Technology*. **55**(4), 221-235 (2012).

- [12] Lewis, M.A., Staruch, R.M. & Chopra, R. Thermometry and ablation monitoring with ultrasound. *International Journal of Hyperthermia*. **31**, 163-181 (2015).
- [13] Fani, F., Saccomandi, P. & Silvestri, S. CT-based thermometry: An overview. *International Journal of Hyperthermia*. **30**, 219-227 (2014).
- [14] Rieke, V. & Pauly, K.B. MR thermometry. *Journal of Magnetic Resonance Imaging*. **27(2)**, 376-390 (2008).
- [15] Petrova, E.V. et al. Using optoacoustic imaging for measuring the temperature dependence of Gruneisen parameter in optically absorbing solutions. *Optics Express*. **21(21)**, 25077-25090 (2013).
- [16] Gao, L. et. al. Single-cell photoacoustic thermometry. *Journal of biomedical optics*. **18(2)**, 026003-026003 (2013).
- [17] Shah, J. et al. Photoacoustic imaging and temperature measurement for photothermal cancer therapy. *Journal of biomedical optics*. **13(3)**, 034024-034024 (2008).
- [18] Yao, L., Huang, H. & Jiang, H. Finite-element-based photoacoustic imaging of absolute temperature in tissue. *Optics letters*. **39**, 5355-5358 (2014).
- [19] Pang, G.A., Bay, E., Deán-Ben, X.L & Razansky, D. Three-dimensional optoacoustic monitoring of lesion formation in real time during radiofrequency catheter ablation. *Journal of cardiovascular electrophysiology*. **26(3)**, 339-345 (2015).
- [20] Gray, J.P. et al. Multi-wavelength photoacoustic visualization of high intensity focused ultrasound lesions. *Ultrasonic imaging*. **38(1)**, 96-112 (2016).
- [21] Larina, I.V., Larin, K.V. & Esenaliev, R.O. Real-time optoacoustic monitoring of temperature in tissues. *Journal of Physics D: Applied Physics*. **38(15)**, 2633-2639 (2005).
- [22] Larin, K.V., Larina, I.V., Motamedi, M. & Esenaliev, R.O. Monitoring of temperature distribution with optoacoustic technique in real time. *SPIE Proc*. **3916**, 311-321 (2000).
- [23] Yao, D., Zhang, C., Maslov, K. & Wang, L.V. Photoacoustic measurement of the Grüneisen parameter of tissue. *Journal of biomedical optics*. **19(1)**, 017007-017007 (2014).
- [24] Deán-Ben, X.L., Ozbek, A. & Razansky, D. Volumetric real-time tracking of peripheral human vasculature with GPU-accelerated three-dimensional optoacoustic tomography. *IEEE transactions on medical imaging*. **32(11)**, 2050-2055 (2013).
- [25] Wang, L.V. & Wu, H. Biomedical optics: principles and imaging. *John Wiley & Sons*. (2012).
- [26] Wang, W. & Mandelis, A. Thermally enhanced signal strength and SNR improvement of photoacoustic radar module. *Biomedical Optics Express*. **5**, 2785-2790 (2014).
- [27] Alexander A. Oraevsky, A.A., Esenaliev, R.O., Motamedi, M., Karabutov, A.A. Real time optoacoustic monitoring of changes in tissue properties. US Patent 6,309,352.
- [28] Niemz, M.H. Laser-tissue interactions: fundamentals and applications. *Springer Science & Business Media*. (2013).
- [29] Deán-Ben, X.L., Gottschalk, S., McLarney, B., Shoham, S., & Razansky, D. Advanced optoacoustic methods and labelling approaches for imaging of multi-scale in vivo dynamics. *Chem Soc Rev* **46**, 2158—2198 (2017).

[30] Chu, K.F. & Dupuy, D.E. Thermal ablation of tumours: biological mechanisms and advances in therapy. *Nature Reviews Cancer* **14**, 199-208 (2014).

[31] Shih, T. et. al. Numerical analysis of coupled effects of pulsatile blood flow and thermal relaxation time during thermal therapy. *International Journal of Heat and Mass Transfer*. **55**, 3763-3773 (2012).